QUARKONIUM DECAYS: TESTING THE 3-GLUON VERTEX

K. KOLLER

Institut für Theoretische Physik, Universität München, W. Germany

K.H. STRENG[1]

SLAC, Stanford University, USA

T.F. WALSH

Deutsches Elektronen-Synchrotron DESY, Hamburg*, W. Germany
and
CERN, Geneva, Switzerland

P.M. ZERWAS

Deutsches Elektronen-Synchrotron DESY, Hamburg,
and
Institut für Theoretische Physik, TH Aachen*, W. Germany

We study the 3-jet decays of S- and P-wave quarkonia with $C = +$. If observed, some of these will offer a way of seeing the 3G vertex of QCD via

$$^1S_0, {}^3P_0, {}^3P_2(Q\bar{Q}) \rightarrow GGG + Gq\bar{q} \rightarrow 3\,\text{jets}.$$

(As is well-known, cancellations reduce $^3P_1(Q\bar{Q}) \rightarrow GGG$.) We elaborate in detail the S-wave decay, as it is expected to show all the characteristic features of orthoquarkonium decays into 4 jets,

$$^3S_1(Q\bar{Q}) \rightarrow GGGG + GGq\bar{q} \rightarrow 4\,\text{jets},$$

which we will comment upon. These quarkonium decays offer a very clear signal for QCD as a non-abelian local gauge field theory with color-charged gluons.

1. Introduction

Quantum chromodynamics' elementary colored quarks and gluons are not directly observable. They are permanently bound in colorless physical states, the hadrons.

---

[1] Kade Fellow.
* Permanent address.

This unobservability of the elementary objects of the theory is not sanctioned by tradition in physics. So we are obliged to look for the cleanest possible (if indirect) experimental evidence for quarks and gluons – particularly gluons. Convincing experimental evidence for these colored vector quanta and their self-interaction would essentially establish the theory. QCD is a non-abelian local gauge theory [1]. It requires that gluons exist and that they interact in a prescribed way with quarks as well as with themselves. The theory becomes free at short distances. This helps, since it means that QCD quanta (or partons) are produced with perturbatively calculable rates in short-distance processes such as e^+e^- annihilation, quarkonium decays or high-p_T hadron production in hadron-hadron collisions. Quarkonium decays are particularly useful. To leading order in the QCD coupling g_s, only gluons are created in the annihilation [1].

Empirically we know that $Y(9.46) = 1^3S_1(b\bar{b})$ decays are well described by the QCD mechanism $(b\bar{b}) \rightarrow GGG \rightarrow 3$ low energy jets [2]. Clean jets are not seen. But distributions do need a matrix element containing vector gluons with color [3]. The next resonance should give very clean multijet decays. Clean jets are seen in $e^+e^- \rightarrow q\bar{q}G \rightarrow 3$ jets at $E_{cm} = 30$ GeV [4]. So a parton with energy $7-10$ GeV will appear as a clearly visible jet of (colorless) hadrons. We take this to be an empirical fact.

The observability of partons as jets makes quarkonium decays an ideal place to look for evidence of gluon self-coupling. QCD predicts that, at short distance, $G \rightarrow GG$ with a calculable rate as a result of this self-coupling. This is analogous to the bremsstrahlung of a gluon by a quark at short distance, $q \rightarrow qG$, or of a photon by an electron in QED, $e \rightarrow e\gamma$. In all these cases the vector quantum has an energy and angle distribution $\propto (dE/E)d\theta/\theta$ at small E and θ. The bremsstrahlung of soft collinear gluons by gluons depends on everything in QCD – a small effective coupling at short distance as well as self-coupled colored vector gluons. (Of course, a clear $(dE/E)d\theta/\theta$ spectrum of jets may need a lot of energy.)

We take up the decay of $C = +$ $(Q\bar{Q})$ bound states (paronium – the word "paraquarkonium" is too long for us). This is shown in fig. 1 up to $O(g_s^3)$,

$$(Q\bar{Q}) \rightarrow GG + GGG + Gq\bar{q} \rightarrow 2 \text{ jets} + 3 \text{ jets}. \qquad (1)$$

It turns out that the diagrams involving the 3G vertex dominate over $Gq\bar{q}$ by an order of magnitude (apart from the exceptional $^3P_1$). Expression (1) is thus a nice analogy to

$$e^+e^- \rightarrow q\bar{q} + q\bar{q}G \rightarrow 2 \text{ jets} + 3 \text{ jets}. \qquad (2)$$

Because of the gluons' self-coupling and large octet color charge in fig. 1, the fraction of 3-jet events in (1) is about $\frac{9}{4}$ of what it is in (2) at the same energy [5]. This, and the characteristic distribution in (1), is what we are looking for.
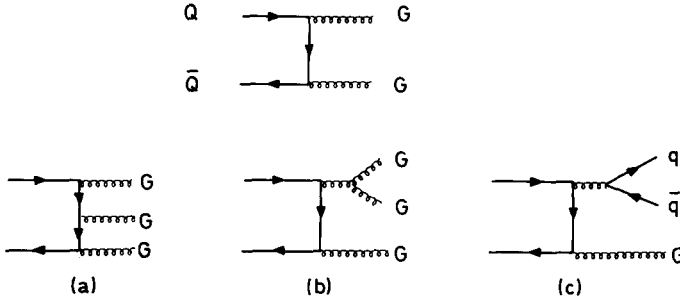
Fig. 1. Paronium decays into GG and GGG, Gq$\bar{q}$ final states. Permutations of gluon lines are not shown. (The GG diagram is absent for $^3P_1$ decays.)

Reaction (1) is difficult to observe experimentally. The $C = +$ ($Q\bar{Q}$) states have to be reached by radiative decay from a $C = -$ $^3S_1$ state produced in e^+e^- annihilation,

$$e^+e^- \to {}^3S_1(Q\bar{Q}) \to \gamma + {}^1S_0(Q\bar{Q})$$

$$\to \gamma + {}^3P_J(Q\bar{Q}), \qquad (3)$$

where $J = 0,1,2$. We are therefore most interested in (1) (particularly the S-wave paronium decay) as a laboratory for methods that we can use to analyse the ground state $^3S_1$ orthonium decay up to order g_s^4, fig. 2,

$$^3S_1(Q\bar{Q}) \to GGG + GGGG + GGq\bar{q}. \qquad (4)$$

This can be observed directly on resonance in e^+e^- annihilation. The differential rate for $(Q\bar{Q}) \to GGG$ is finite everywhere. Divergences occur for GGGG when a gluon is soft or parallel to another. (GGq$\bar{q}$ has a divergence for parallel q$\bar{q}$ but not for soft quarks; we expect this final state to be swamped by GGGG.) This behavior is due again to the 3G vertex of QCD. We will discuss (4) in detail in a subsequent paper.
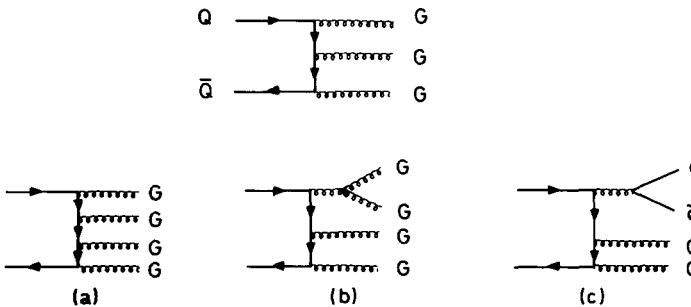

Fig. 2. Generic diagrams of orthoquarkonium decays into 3G and 4G, GGq$\bar{q}$ final states.

All our calculations are for tree graphs. Since $(Q\overline{Q}) \to GGG$ in (1) is small compared to $Q\overline{Q} \to GG$, it is consistent to ignore loop corrections to the latter. We want to check the ratio of 3- to 2-jet events in (1), compared to (2). This measures the strength of the 3G vertex. (3-jet distributions check the bremsstrahlung character of $G \to GG$.) The 3G strength is this ratio, up to corrections of order $\alpha_s = g_s^2/4\pi$. This is tolerable, since we are looking for a factor $\frac{9}{4}$ in (1) compared to (2). (This does assume that radiative corrections to $(Q\overline{Q})$ decay are not too big. Some corrections are big, but the overall effect does not appear too serious [6]*.)

Our main conclusion is that most $C = +$ (QQ) decays (if observed) do provide a clean check on the 3G vertex of QCD. We calculate helicity amplitudes for physical gluon polarization. So there is no gauge ambiguity in the association of specific graphs to specific amplitudes. The diagram in fig. 1 with all gluons attached to a heavy fermion line has no divergence for S-wave $(Q\overline{Q})$. We already remarked that $q\overline{q}$ production is swamped by the gluon diagrams involving the 3G vertex. These thus dominate.

The $1^{++}\,{}^3P_1(Q\overline{Q})$ decay is an exception [7]. $(Q\overline{Q}) \to GG$ is forbidden by an analog of Yang's theorem. $(Q\overline{Q}) \to GGG$ is tiny due to cancellations and $(Q\overline{Q}) \to Gq\overline{q}$ turns out to dominate. Paronium decays do not automatically check the 3G vertex. The structure of the short-distance source is important, and the individual cases have to be calculated.

The general characteristics of the higher order 0^{-+} paronium S-wave decay are expected to be closely analogous to those of the 1^{--} orthonium S-wave decay, experimentally much more easily accessible in e^+e^- collisions. S-wave decays are the only decays where $G \to q\overline{q}$ and (the even bigger) $G \to GG$ gluon splitting dominate over diagrams with all gluons attached to a heavy fermion line, everywhere in phase space. They are the only decays where the development of hadron distributions with increasing quarkonium mass [8] can be derived from Altarelli-Parisi type equations [9].

The three-parton decays of $C = +$ onia have been studied previously by Barbieri, Caffo and Remiddi [6]. Where we overlap, we have checked that our results agree with theirs.

In sect. 2 we present the helicity amplitude method. We consider the kinematics, the consequences of symmetries on the amplitudes, and the $(Q\overline{Q})$ Bethe-Salpeter bound-state amplitudes. Sect. 3 contains the helicity analysis of S-wave ${}^1S_0(Q\overline{Q}) \to GG$ and ${}^3S_1(Q\overline{Q}) \to GGG$ decays and also P-wave ${}^3P_0$, ${}^3P_2(Q\overline{Q}) \to GG$ decays. Sect. 4 contains our results on paronium decays to GGG and $Gq\overline{q}$. We also comment on orthonium decays to GGGG, based on the general structure of the S-wave $(Q\overline{Q})$ decays. Sect. 5 contains results on ${}^3P_0$, ${}^3P_2 \to 2$ jets + 3 jets, and sect. 6 is a summary and outlook.

---

* For 3-parton decays see the third of these papers.

2. The helicity method

In this paper we calculate helicity amplitudes for GG and GGG, G$q\bar{q}$ decays of $(Q\bar{Q})$ [10]. Squared and summed over helicities, these give rates. It is not necessary to introduce unphysical degrees of freedom (ghosts). Another advantage of this method is that we can calculate gluon polarizations, if desired. In this section we simply summarize information we will need for the actual calculations.

The matrix element for decay of a color singlet $(Q\bar{Q})$ to GG (colors a and b) is proportional to δ_{ab}. For $C = +$ $(C = -)$ GGG decays (colors a, b, c) the matrix element is proportional to f_{abc} (d_{abc}). Time-reversal invariance requires all matrix elements to be relatively real in Born approximation; we will choose them real. From now on, a, b, c refer to color indices and k_i, $\lambda_i = \pm 1$ to gluon momenta and helicities. Decay matrix elements [e.g. for $(Q\bar{Q}) \to$ GG] are written

$$T_{S_z}^{ab}(k_1, \lambda_1; k_2, \lambda_2),$$

where S_z labels in addition the z-component of spin of the $(Q\bar{Q})$ state, the z-axis defined by k_1. Parity, angular momentum and Bose symmetry now give the following constraints on the T's.

$(Q\bar{Q}) \to$ GG decays. Parity requires that

$$T_{S_z}^{ab}(k_1, \lambda_1; k_2, \lambda_2) = n T_{-S_z}^{ab}(k_1, -\lambda_1; k_2, -\lambda_2), \tag{5}$$

where $n = \eta(-)^s$ is the normality of the $(Q\bar{Q})$ state of parity η and spin s. Angular momentum requires that

$$T_{S_z}^{ab}(k_1, \lambda_1; k_2, \lambda_2) \neq 0, \qquad \text{only if } S_z = \lambda_1 - \lambda_2. \tag{6}$$

Bose symmetry for on-shell gluons G gives

$$T_{S_z}^{ab}(k_1, \lambda_1; k_2, \lambda_2) = (-)^{S - S_z} T_{-S_z}^{ba}(k_1, \lambda_2; k_2, \lambda_1). \tag{7}$$

$(Q\bar{Q}) \to$ 3G decays. In this case parity gives

$$T_{S_z}^{abc}(k_1, \lambda_1; k_2, \lambda_2; k_3, \lambda_3) = -n(-)^{S_z} T_{-S_z}^{abc}(k_1, -\lambda_1; k_2, -\lambda_2; k_3, -\lambda_3). \tag{8}$$

There is no constraint analogous to (6), but Bose symmetry gives

$$T_{S_z}^{abc}(k_1, \lambda_1; k_2, \lambda_2; k_3, \lambda_3) = -(-)^{S_z} T_{S_z}^{acb}(k_1, \lambda_1; k_3', \lambda_3; k_2', \lambda_2), \tag{9}$$

where k_i' is related to k_i $(i = 2, 3)$ by a rotation of 180° around k_1. If $S = 0$, (9) holds for interchanges of all particles, including particle 1.

$(Q\overline{Q}) \to Gq\overline{q}$ decay.   The only constraint arises from parity invariance,

$$T_{S_z}^a(k_1, \lambda_G; p, \lambda_q; \bar{p}, \lambda_{\bar{q}}) = -n(-)^{S_z - \lambda_q - \lambda_{\bar{q}}} T_{-S_z}^a(k_1, -\lambda_G; p, -\lambda_q; \bar{p}, -\lambda_{\bar{q}}),$$

(10)

where quark (antiquark) momenta and helicities are $p, \lambda_q, \bar{p}, \lambda_{\bar{q}}$. We do not explicitly label quark colors.

The decay amplitude for a quarkonium state to some final state F is (fig. 3)

$$T = \left[\frac{2M}{(2\pi)^3} \right]^{1/2} \int d^4q \, \mathrm{Tr}[\mathfrak{M}\Psi].$$

(11)

$\mathfrak{M}$ is the $Q\overline{Q} \to F$ Feynman amplitude (without spinors for $Q, \overline{Q}$), and Ψ is the bound-state Bethe-Salpeter amplitude in the quarkonium rest frame,

$$\Psi = \frac{1}{4m^2}[m + \tfrac{1}{2}\not{P} + \not{q}]\frac{1 + \gamma^0}{2}\not{E}[m - \tfrac{1}{2}\not{P} + \not{q}],$$

(12)

where P is the momentum of the $(Q\overline{Q})$ state, M its mass and m the quark mass $(= \tfrac{1}{2}M$ in the static approximation).

The wave functions of the bound state for S- and P-waves are [11]:
S-wave:

$$\not{E}(0^{-+}) = \sqrt{\tfrac{1}{2}}\,\gamma_5 \frac{R_0(q^2)}{\sqrt{4\pi}}\delta(q^0),$$

(13)

$$\not{E}(1^{--}) = \sqrt{\tfrac{1}{2}}\not{E}(S_z)\frac{R_0(q^2)}{\sqrt{4\pi}}\delta(q^0);$$

(14)

P-wave:

$$\not{E}(0^{++}) = \sqrt{\tfrac{1}{2}}\not{q}_E \frac{R_1(q^2)}{\sqrt{4\pi}}\delta(q^0),$$

(15)

$$\not{E}(1^{++}) = \sqrt{\frac{3}{4}}\,\frac{1}{M}\varepsilon_{\mu\nu\rho\sigma}\epsilon^\mu(S_z)q_E^\nu p^\rho p^\sigma \frac{R_1(q^2)}{\sqrt{4\pi}}\delta(q^0),$$

(16)

$$\not{E}(2^{++}) = \sqrt{\tfrac{3}{2}}\,\varepsilon_{\mu\nu}(S_z)\gamma^\mu q_E^\nu \frac{R_1(q^2)}{\sqrt{4\pi}}\delta(q^0).$$
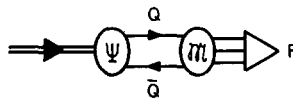
(17)

Fig. 3. Decay amplitude for a quarkonium state $(Q\overline{Q})$ to some final state F.

The notation is as follows. $\varepsilon^\mu(S_z)$ and $\varepsilon^{\mu\nu}(S_z)$ are conventional polarization vector and tensor. $R_{0,1}(q^2)$ are the radial wave functions in momentum space. The normalization is

$$\int d^3q R^2_{0,1}(q^2) = 4\pi. \tag{18}$$

$q_E = (0, \boldsymbol{q}_E)$ is a unit vector in the direction of q.

In calculating rates for non-relativistic $(Q\bar{Q})$ we will take only the lowest terms in an expansion of $\mathfrak{M}$ in powers of q. Then we encounter for S- and P-waves the integrals

$$\int \frac{d^3q}{(2\pi)^{3/2}} R_0(q^2) = R_0(0) = \sqrt{4\pi}\,\phi(0),$$

$$\int \frac{d^3q}{(2\pi)^{3/2}} q^i q^j_E R_1(q^2) = \delta^{ij} \frac{d}{dr} R_1(r)\Big|_{r=0} = \delta^{ij} R'_1(0), \tag{19}$$

where $\phi(0)$ is the wave function at the origin and $R_0(0)$, $R'_1(0)$ are the S-wave radial wave function at $r=0$ and the derivative of the P-wave radial wave function at the origin.

If S_z is the z-component of spin of the $(Q\bar{Q})$ state and θ and ϕ the polar and azimuthal angles of the $(Q\bar{Q}) \to GG$ axis (or of the thrust axis for $(Q\bar{Q}) \to GGG + Gq\bar{q}$ with χ the azimuthal angle of the three-parton plane about this axis), then the angular dependence of $\mathfrak{M}$ is given by

$$\mathfrak{M}(\theta, \phi) = \sum_{S'_z} T_{S'_z}(k_1\lambda_1, k_2\lambda_2) d^S_{S_z S'_z}(\theta) e^{i\phi(S_z - \lambda_1 + \lambda_2)} \tag{20}$$

for $(Q\bar{Q}) \to GG$ and

$$\mathfrak{M}(\theta, \phi, \chi) = \sum_{S'_z} T_{S'_z}(k_1\lambda_1, k_2\lambda_2, k_3\lambda_3) d^S_{S_z S'_z}(\theta) e^{i\phi S_z + i\chi S'_z} \tag{21}$$

for $(Q\bar{Q}) \to GGG + Gq\bar{q}$. Of course, there is no angular dependence of the rate for $S = 0$ or spin averaged $S = 1, 2$.

The decay rates are

$$d\Gamma = \frac{1}{2M} \frac{|\mathfrak{M}|^2}{32\pi^2} \frac{d\Omega}{(2!)}, \tag{22}$$

for $(Q\bar{Q}) \to GG$ and

$$d\Gamma = \frac{1}{2M} \frac{|\mathfrak{M}|^2}{8(2\pi)^5} \frac{dx_1 dx_2 d\cos\theta d\phi d\chi}{(3!)}, \tag{23}$$

for $(Q\bar{Q}) \to GGG$ and $q\bar{q}G$.

3. Lowest order decays

Decay rates and distributions are well-known in this case [1]. We recapitulate these results here in the helicity formalism.

$^1S_0 = 0^{-+} \to GG$.

$$T^{ab}(++) = \frac{2}{\sqrt{3}} \frac{4\pi\alpha_s}{\sqrt{M}} \frac{R_0(0)}{\sqrt{4\pi}} \delta^{ab},$$

$$\Gamma(GG) = \frac{8}{3} \frac{\alpha_s^2}{M^2} |R_0(0)|^2. \tag{24}$$

The amplitude $T_{ab}(--) = -T_{ab}(++)$ by parity; all other combinations vanish by angular momentum conservation. From now on we will only list independent amplitudes which are not trivially constrained to vanish.

$^3P_0 = 0^{++} \to GG$.

$$T^{ab}(++) = 4\sqrt{3} \frac{4\pi\alpha_s}{M^{3/2}} \frac{R_1'(0)}{\sqrt{4\pi}} \delta^{ab},$$

$$\Gamma(GG) = \frac{96\alpha_s^2}{M^4} |R_1'(0)|^2. \tag{25}$$

$^3P_2 = 2^{++} \to GG$. It turns out that the $S_z = \Delta\lambda = 0$ amplitude vanishes, so that only $S_z = \Delta\lambda = 2$ is populated:

$$T_{+2}^{ab}(+-) = 4 \frac{4\pi\alpha_s}{M^{3/2}} \frac{R_1'(0)}{\sqrt{4\pi}} \delta^{ab},$$

$$\Gamma(GG) = \frac{128}{5} \frac{\alpha_s^2}{M^4} |R_1'(0)|^2. \tag{26}$$

$^3S_1 = 1^{--} \to GGG$. In this case we write

$$T_{S_z}^{abc}(\lambda_1, \lambda_2\lambda_3) = \frac{2}{\sqrt{3}} \frac{(4\pi\alpha_s)^{3/2}}{M^{1/2}} \frac{R_0(0)}{\sqrt{4\pi}} d^{abc} a_{S_z}(\lambda_1, \lambda_2\lambda_3)$$

(our notation reflects that k_1 defines the spin quantization axis of the decaying

resonance), where

$$a_+(+,++)=0,$$

$$a_+(+,+-)=(1-x_2)(1-x_3)/x_1^2 x_2 x_3,$$

$$a_+(+,--)=(1-x_1)/x_2 x_3,$$

$$a_+(-,++)=0,$$

$$a_+(-,+-)=(1-x_1)(1-x_2)^2/x_1^2 x_2 x_3,$$

$$a_0(+,++)=a_0(+,--)=0,$$

$$a_0(+,+-)=\sqrt{2}\,(1-x_3)\sqrt{(1-x_1)(1-x_2)(1-x_3)}\,/x_1^2 x_2 x_3,$$

$$\Gamma(\mathrm{GGG})=\frac{40(\pi^2-9)}{81\pi}\frac{\alpha_s^3}{M^2}|R_0(0)|^2. \tag{27}$$

The x_i are the gluon energies in units of the beam energy. It is obvious from (27) that all amplitudes are finite for any $x_i \to 0$. This is due to spin conservation. The matrix element for emission of a soft transverse gluon is $\propto u^+\gamma_\perp u \to 0$ as $|p_G| \to 0$. This cancels the divergence of an attached propagator for $|p_G| \to 0$. The amplitude is finite in this limit.

For unpolarized leptons, $e^+e^- \to 1\gamma \to (Q\overline{Q}) \to 3G$, the angular distribution of the 3G state can be written [12]

$$\frac{4\pi}{\Gamma}\frac{\mathrm{d}\Gamma}{\mathrm{d}x_1\mathrm{d}x_2\mathrm{d}R}=\frac{27}{8(\pi^2-9)}\left\{\sigma_U(1+\cos^2\theta)+2\sigma_L\sin^2\theta\right.$$

$$\left.+2\sigma_T\sin^2\theta\cos 2\chi-2\sqrt{2}\,\sigma_I\sin 2\theta\cos\chi\right\},$$

$$\sigma_U=\tfrac{4}{3}\left\{x_1^2(1-x_1)^2+x_2^2(1-x_2)^2+x_3^2(1-x_3)^2\right\}/x_1^2 x_2^2 x_3^2-\sigma_L,$$

$$\sigma_L=2\sigma_T=\tfrac{8}{3}\left\{(1-x_2)^2+(1-x_3)^2\right\}(1-x_1)(1-x_2)(1-x_3)/x_1^4 x_2^2 x_3^2,$$

$$\sigma_I=\tfrac{2}{3}\sqrt{2}\left[(1-x_1)(1-x_2)(1-x_3)\right]^{1/2}$$

$$\times\left\{(1-x_2)(1-x_3)(x_2-x_3)+(1-x_1)\left[(1-x_2)^3-(1-x_3)^3\right]\right\}/x_1^4 x_2^2 x_3^2,$$

$$\tag{28}$$

where $dR = d\cos\theta\, d\chi$. θ is the angle between x_1 and the e^+e^- beam. χ is the azimuthal angle between the x_2-x_3 plane and the beam. This is responsible for the asymmetric appearance of (28).

4. $^1S_0(Q\bar{Q})$ decay to 3 jets; remarks on $^3S_1 \rightarrow$ 4 jets

The paronium $^1S_0$ state can decay in next order (g_s^3 in amplitude) to GGG and Gq$\bar{q}$,

$$
^1S_0(Q\bar{Q}) \rightarrow \begin{cases} GG & (g_s^2) \\ GGG + Gq\bar{q} & (g_s^3) \\ \vdots \end{cases}
\tag{29}
$$

We will not discuss g_s^4 corrections to the GG decay amplitude [6].

We consider the GGG decay first.

$(Q\bar{Q}) \rightarrow GGG$

Since we calculate helicity amplitudes, it is possible to separate the contribution involving the 3G vertex (b amplitude in fig. 1) from that which does not, fig. 1a. For transverse physical gluon polarizations there is no gauge dependence which might mix diagrams a and b. This is obvious, since there is no possible gauge dependence of a arising from the G propagator. The gluon propagator appears only in b, introducing an apparent gauge-dependent term in the Landau gauge. This term vanishes, however, for on-shell final gluons with physical polarization (as it must if the sum of a and b is to be gauge independent).

The 3G decay amplitude is now⋆

$$
T^{abc}(\lambda_1, \lambda_2\lambda_3) = -\sqrt{\frac{2}{3}} \frac{(4\pi\alpha_s)^{3/2}}{M^{1/2}} \frac{R_0(0)}{\sqrt{4\pi}} f^{abc}[a(\lambda_1, \lambda_2\lambda_3) + b(\lambda_1, \lambda_2\lambda_3)],
\tag{30}
$$

where

$$
a(+,++) = 0,
$$

$$
b(+,++) = \frac{x_1 x_2 x_3 + (1-x_1)(1-x_2)(1-x_3)}{x_1 x_2 x_3 \sqrt{(1-x_1)(1-x_2)(1-x_3)}},
$$

$$
a(+,+-) = -\frac{2(1-x_1)\sqrt{(1-x_1)(1-x_2)(1-x_3)}}{x_1 x_2 x_3},
$$

$$
b(+,+-) = \frac{(1-x_1)^2[(1-x_2)(1-x_3) - x_1(1-x_1)]}{x_1 x_2 x_3 \sqrt{(1-x_1)(1-x_2)(1-x_3)}}.
\tag{31}
$$

⋆ Our Feynman rules are those of ref. [13].

All other amplitudes follow by parity or Bose symmetry. (The color f coupling allows for the decay $0^{-+} \to G^a G^b G^c$ in non-abelian theories; the corresponding decay for abelian theories would be forbidden by C conjugation.)

The amplitudes behave as expected. The a's are finite everywhere on the Dalitz plot. They have no infrared ($x_i \to 0$) or collinear ($x_i \to 1$) divergences. The reason is the same as for $1^{--} \to GGG$: The divergences from propagators are cancelled by recoil factors for soft emission from a non-relativistic Q. The b amplitudes show soft ($x_i \to 0$) and collinear ($x_i \to 1$) divergences, arising from the G propagator in fig. 1b. To this order the divergent parts factorize into a $(Q\bar{Q}) \to GG$ amplitude and $G \to GG$ (which contains the soft and collinear divergences). This proves that one can use Altarelli-Parisi equations for jet development on S-wave resonances.

The functions $a(+,++)$ and $b(+,++)$, showing the most interesting structure of all helicity amplitudes, are plotted in fig. 4; the Dalitz-plot density is shown in fig. 5. The overall thrust distribution,

$$\frac{1}{\Gamma_{LO}(GG)} \frac{d\Gamma(GGG)}{dT} = \frac{\alpha_s}{\pi} \frac{3}{2} \int_{2(1-T)}^{T} dx_2 \sum_{\lambda_i} |a(\lambda_1,\lambda_2\lambda_3) + b(\lambda_1,\lambda_2\lambda_3)|^2_{x_1=T},$$
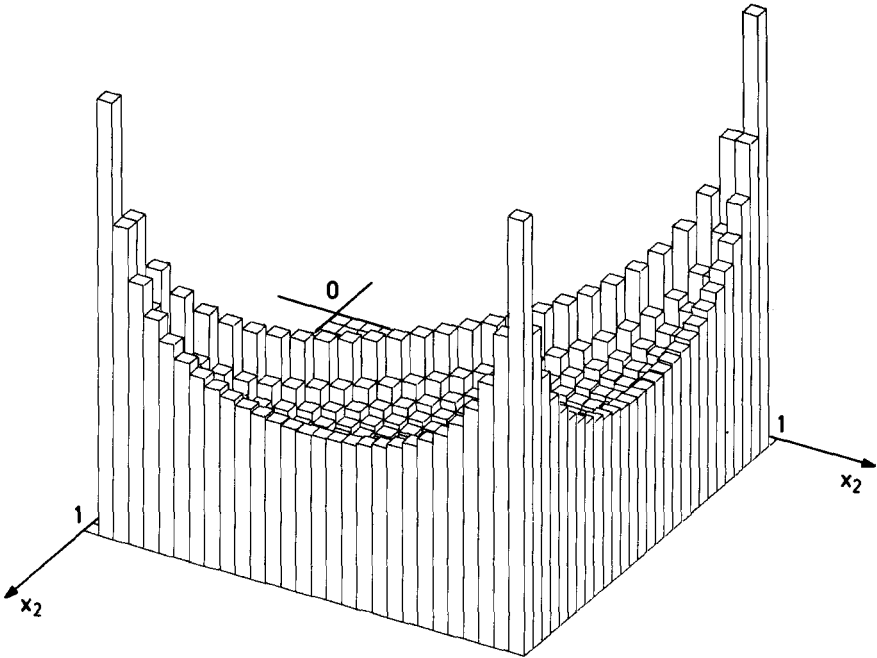
(32)

Fig. 4. The b amplitude (measuring the 3-gluon coupling) in the paronium decay $0^{-+}(Q\bar{Q}) \to G(+)G(+)G(+)$ into polarized gluons; the a amplitude (all gluons attached to the heavy quark line) vanishes for these helicities.
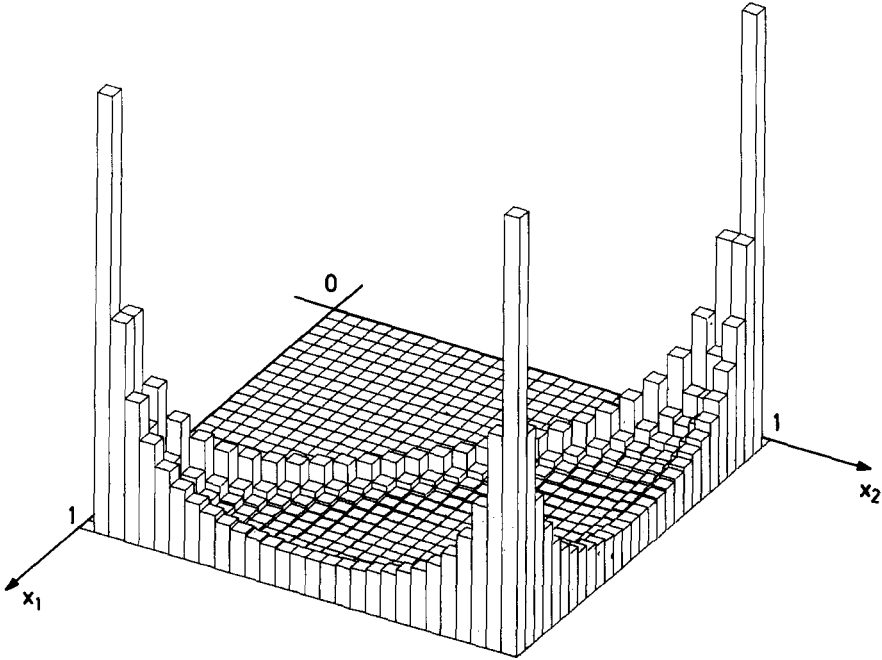
Fig. 5. Dalitz-plot density for $0^{-+}(Q\overline{Q}) \to GGG$, sum over all gluon polarizations.

is shown in fig. 6. The 3G vertex contribution is about an order of magnitude or more larger than the a contribution for most T values. The 3G vertex part gives the $T \to 1$ divergent piece

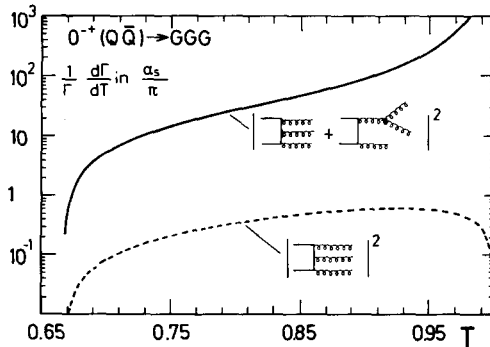$$\frac{1}{\Gamma_{LO}(GG)} \frac{d\Gamma(GGG)}{dT} \sim \frac{\alpha_s}{\pi} \frac{(-6)}{(1-T)} \log(1-T).$$

Fig. 6. Thrust distribution $(1/\Gamma_{LO}(GG))d\Gamma(GGG)/dT$ for $0^{-+}(Q\overline{Q}) \to GGG$ in units of α_s/π (full line); separately shown is the contribution of $|a|^2$, all gluons attached to the heavy quark line. The contribution of the 3-gluon coupling, $|b|^2$, is almost identical to the total thrust distribution.

We can also compare mean values of powers of $1 - T$ for the GGG final state and $e^+e^- \to q\bar{q}G$,

$$
\begin{array}{ccc}
 & \text{GGG} & \text{q}\bar{\text{q}}\text{G} \\[2mm]
\langle(1 - T)\rangle = & 2.63\dfrac{\alpha_s}{\pi} & 1.05\dfrac{\alpha_s}{\pi} ,
\end{array}
\tag{33}
$$

$$
\begin{array}{ccc}
\langle(1 - T)^2\rangle = & 0.26\dfrac{\alpha_s}{\pi} & 0.095\dfrac{\alpha_s}{\pi} .
\end{array}
\tag{34}
$$

The results for GGG agree with ref. [6]. The corresponding number for a static 3G source [14] is

$$
\langle(1 - T)\rangle = 2.59\frac{\alpha_s}{\pi} .
$$

We find the largest contribution from the $b(+, ++)$ amplitude. There is a smaller contribution from $b(+, + -)$ and a negligible one from $b(+, - -)$. This coincides with what one expects for the $G \to GG$ fragmentation functions. That for $+ \to + +$ is $\propto [z^{-1} + (1 - z)^{-1}]$, that for $+ \to + -$ is $\propto [(1 - z)^{-1} - 1]$ and $+ \to - -$ vanishes. (Here z is the momentum of a bremsstrahlung gluon). This explains why the thrust distribution for $+ - -$ is finite at $T = 1$. It is somewhat surprising, however, that the pattern of the bremsstrahlung spectra persists over the entire thrust region. This is shown in detail in fig. 7 for all unrelated helicity cross sections*.

$(Q\bar{Q}) \to q\bar{q}G$

It will not be easy to distinguish quark and gluon jets. So we must consider $Q\bar{Q} \to q\bar{q}G$ together with GGG. The $q\bar{q}G$ process has only a collinear singularity (no soft infrared divergence). It is also smaller than GGG by a parton color charge factor. The amplitude for $(Q\bar{Q}) \to G^a(\lambda_G)q^i(\lambda_q)\bar{q}^j(\lambda_{\bar{q}})$ $(a, i, j = \text{color indices})$ factorizes into the decay amplitude $(Q\bar{Q}) \to G^a(\lambda_G)G^b(\lambda^*)$ and the decay of the virtual gluon $G^b(\lambda^*) \to q^i(\lambda_q)\bar{q}^j(\lambda_{\bar{q}})$, see fig. 1c. Taking the real gluon's momentum as the spin quantization axis we have for arbitrary quarkonium spin

$$
T\{(Q\bar{Q})_{S_z} \to G^a(\lambda_G)q^i(\lambda_q)\bar{q}^j(\lambda_{\bar{q}})\}
$$

$$
= T\{(Q\bar{Q})_{S_z} \to G^a(\lambda_G)G^a(S_z - \lambda_G)^*\}
$$

$$
\times \frac{1}{4(1 - x_G)} T\{G^a(S_z - \lambda_G)^* \to q^i(\lambda_q)\bar{q}^j(\lambda_{\bar{q}})\} .
\tag{35}
$$

---

* The others are related to those shown in the figures by parity invariance and Bose symmetry.
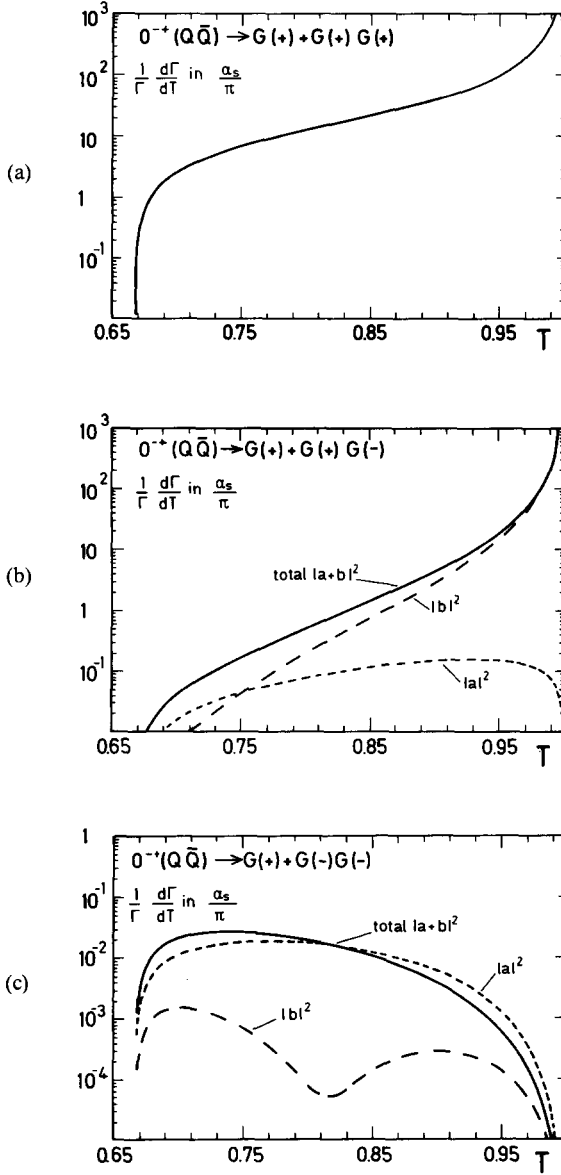
Fig. 7. Dependence of the thrust distribution for $0^{-+}(Q\bar{Q}) \rightarrow G(\lambda_1) + G(\lambda_2)G(\lambda_3)$ on the helicities λ_i of the gluons; $G(\lambda_1)$ denotes the most energetic gluon. (a) $0^{-+}(Q\bar{Q}) \rightarrow G(+) + G(+)G(+)$; (b) $\rightarrow G(+) + G(+)G(-)$; (c) $\rightarrow G(+) + G(-)G(-)$. All other polarization states are related to these by parity and Bose symmetry. Separately shown are the contributions of the a amplitude (dotted line), the b amplitude (dashed line) and the total distribution (full line).

The matrix element of the virtual gluon decay is, in units of $g(\frac{1}{2}\lambda_{ij}^a)m_Q$,

$$
T_{\lambda^*}(\lambda_q\lambda_{\bar{q}}) = \begin{cases} 2\sqrt{2}\sqrt{1-x_G}\left(1-x_{\bar{q}/q}\right)/x_G, & \text{for } \lambda^*\lambda_q = +\tfrac{1}{2}/-\tfrac{1}{2}, \\ \mp 4\sqrt{(1-x_G)(1-x_q)(1-x_{\bar{q}})}\,/x_G, & \text{for } \lambda^* = 0 \text{ and } \lambda_q = \pm\tfrac{1}{2}. \end{cases}
$$

(36)

Note that the latter result is just twice the transverse momentum of the quark relative to the gluon's momentum. Quark and antiquark always carry opposite helicities, $\lambda_q\lambda_{\bar{q}} = -\frac{1}{4}$ for vector coupling.

The matrix element for paronium decay $0^{-+} \rightarrow GG^*$ is just a constant, independent of the gluon energy, and we finally obtain

$$
T\{0^{-+}(Q\bar{Q}) \rightarrow G^a(\pm)q^i(\lambda_q)\bar{q}^j(\lambda_{\bar{q}})\} = \pm\frac{1}{4\sqrt{3}}\frac{(4\pi\alpha_s)^{3/2}}{M^{1/2}}\frac{R_0(0)}{\sqrt{4\pi}}\lambda_{ij}^a\frac{T_{\pm}(\lambda_q,\lambda_{\bar{q}})}{(1-x_G)}\,.
$$

(37)

We have calculated the thrust distribution for $Gq\bar{q}$, and show its contribution in fig. 8. In the interesting thrust region it is almost an order of magnitude down compared to GGG, even for 5 "light" quark flavors (u,d,s,c,b).

$^3S_1(Q\bar{Q}) \rightarrow 4$ *jets*

From the discussion so far we can already draw some naive inferences about the S-wave decay to 4 jets,

$$
{}^3S_1(Q\bar{Q}) \rightarrow GGGG + GGq\bar{q}.
$$

(38)

For two of the gluons (or $q\bar{q}$) having low invariant mass we expect that this can be factorized into

$$
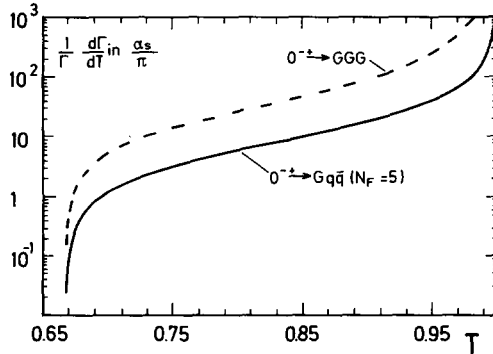{}^3S_1 \rightarrow GGG^* \text{ times } G^* \rightarrow GG \text{ or } q\bar{q},
$$

(39)

Fig. 8. Thrust distribution of $0^{-+}(Q\bar{Q}) \rightarrow Gq\bar{q}$ (5 light quark flavors) compared with GGG.

where the G* can be taken real, $(Q\overline{Q}) \rightarrow GGG$. $G^* \rightarrow GG$ or $q\overline{q}$ follows then from the usual Altarelli-Parisi fragmentation functions, P_{GG} and $P_{q\overline{q}}$ [9]. As shown for paronium decays, we expect the GGGG final state to dominate strongly over $GGq\overline{q}$ decays.

We just want to add one simple remark on the angular correlation between the plane defined by the low mass $G^* \rightarrow GG$ and $q\overline{q}$ fragmentation and the plane of the two hard gluons in (39) [15]. We have already calculated the $^3S_1 \rightarrow GGG$ helicity amplitudes. These define the state of linear polarization of the G^* in (39),

$$\frac{d\Gamma}{dx_1 dx_2 d\psi} \sim 1 + \rho(x_1, x_2, x_3)\cos 2\psi, \tag{40}$$

where, in the notation of ref. [15],

$$\rho = \frac{X_1 X_2 X_3}{X_1^2 + X_2^2 + X_3^2} \tag{41}$$

with $X_1 = 2(1 - x_1)/x_2 x_3$ etc.; ψ is the angle between the polarization vector and the normal to the plane of the two real gluons. ($\rho = \frac{1}{2}$ for "Mercedes stars".) Denoting the momentum of one of the gluon jets in $G^* \rightarrow GG$ by z the angle between this gluon and the G^* polarization vector by χ, we find for the χ-dependent fragmentation functions

$$P_{GG}(z, \chi) = \frac{6}{2\pi}\left[\frac{(1 - z + z^2)^2}{z(1-z)} + z(1-z)\cos 2\chi\right], \tag{42}$$

whereas the fragmentation function for N_F quark flavors in $G^* \rightarrow q\overline{q}$ reads

$$P_{q\overline{q}}(z, \chi) = \frac{1}{2\pi}\frac{N_F}{2}\left[z^2 + (1-z)^2 - 2z(1-z)\cos 2\chi\right]. \tag{43}$$

The resulting angular asymmetry of the broad $G^* \rightarrow GG$ jet pair with respect to the normal of the two thin GG jets is therefore

$$\langle\cos 2\psi\rangle \propto (3 - N_F)z(1-z)\rho. \tag{44}$$

We expect 4–5 active flavors in (44), so that there is a net ψ asymmetry. Note that the $G^* \rightarrow GG$ fragmentation channel just reverses the sign of the asymmetry due to the $q\overline{q}$ channel for $N_F \geqslant 3$. The major axis of broad $G^* \rightarrow GG$ jet pair prefers to be perpendicular to the major axis of the two thin G jet plane.

$^3S_1(Q\overline{Q}) \rightarrow \gamma + 3$ jets

Another way of looking for the 3G vertex is through the radiative decay (fig. 9)

$$(Q\overline{Q}) \rightarrow \gamma GG + \gamma GGG + \gamma Gq\overline{q}. \tag{45}$$
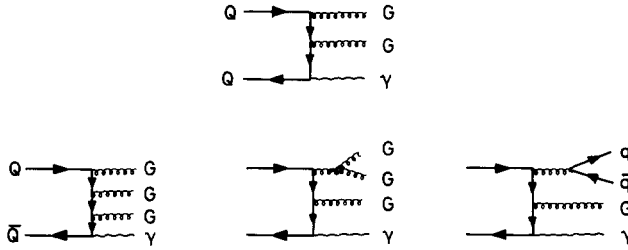
Fig. 9. Generic diagrams of orthoquarkonium decays into $\gamma + GG$ and $\Gamma + GGG$, $\Gamma + Gq\bar{q}$ final states.

For a high mass $(t\bar{t})$ toponium state the $\gamma GG/GGG$ ratio in the Born approximation is

$$\frac{\Gamma(\gamma GG)}{\Gamma(GGG)} = \frac{16\alpha}{5\alpha_s} = 20\%, \tag{46}$$

for $\alpha_s = 0.12$. This is not small.

The mass M of the multijet system in (45) can be tuned by varying the γ energy,

$$M^2 = \left(1 - \frac{2E_\gamma}{M_{t\bar{t}}}\right) M_{t\bar{t}}^2. \tag{47}$$

Since E_γ is known, one can boost into the rest frame and examine events in this frame as a function of M (fig. 10). This provides a close analogy to gluon bremsstrahlung in

$$e^+e^- \rightarrow q\bar{q} + q\bar{q}G. \tag{48}$$

From (42), (43) we see at once that $G \rightarrow GG$ will dominate $G \rightarrow q\bar{q}$ in (45) by a factor $\gtrsim 10$ for $z \lesssim \frac{1}{2}$. Thus initially back-to-back low-M GG jets in (45) should be seen to broaden faster than in (48) due to the factor $\frac{9}{4}$ larger squared color charge of gluons [5].

For $M_{t\bar{t}} \sim 40-50$ GeV it appears quite possible to cover the M range $15-30$ GeV at which (48) has been studied by PETRA. The events will have a clean signature, which makes up for the lower rate, (46).

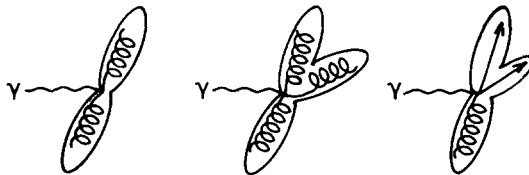We will consider (38) and (45) in more detail in a subsequent paper.

Fig. 10. Jet broadening of $(Q\bar{Q}) \rightarrow \gamma + GG$ in the GG rest frame due to gluon bremsstrahlung $G \rightarrow GG$ and gluon splitting $G \rightarrow q\bar{q}$.

5. P-wave decays

We have discussed S-wave paronium at length because they are straightforward, conceptionally simple and reflect the characteristic features of orthonium decay. P-wave decays are less so. For S-waves to order g_s^3, gluon radiation from the heavy fermion line produces no infrared or collinear divergences. These come from gluon splitting à la Altarelli and Parisi [9]. This is no longer true for P-wave decays.

$^3P_1 \to GGG = Gq\bar{q}$

The P-wave decay $^3P_1 \to GGG + Gq\bar{q}$ is known to be somewhat bizarre [7]. There are remarkable cancellations. For example, we find that for the $+++$ helicity final state, *both* the a and b amplitudes are infrared divergent (i.e. radiation from the heavy fermion line and the gluon splitting diagram). However, amazingly,

$$a\left(^3P_1 \to +++\right) + b\left(^3P_1 \to +++\right) = 0. \qquad (49)$$

For helicities $++-$ the a and b amplitudes are again infrared divergent and the sum is small and finite (not zero this time). The $+--$ amplitudes are finite and small. The absence of infrared divergences for $^3P_1 \to GGG$ can be understood [13], though the numerical smallness of this channel is less trivial (see the discussion below). Fig. 11 shows the $^3P_1 \to GGG$ thrust distribution with the square of the a amplitudes and b amplitudes shown together with the square of their sum. The cancellation is everywhere at least a factor 20 in $d\Gamma/dT$. This cancellation is, of course, a result of the 3G vertex. Nevertheless, we cannot explore $^3P_1$ decays for *direct* experimental evidence of the 3G vertex. The dominant decay is $^3P_1 \to Gq\bar{q}$ with logarithmic width [7]

$$\Gamma_{\ln}\left(^3P_1 \to q\bar{q}G\right) = \frac{N_F}{3} \frac{128}{3\pi} \frac{\alpha_s^3}{M^4} |R_1'(0)|^2 \ln R_c M. \qquad (50)$$

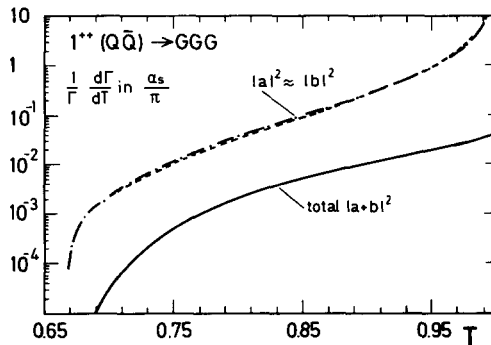Fig. 12 compares the $Gq\bar{q}$ and GGG final state thrust distributions.

Fig. 11. Thrust distribution of $1^{++}(Q\bar{Q}) \to GGG$. Shown are the square of the a amplitude (and the almost identical b amplitude) and the square of the sum $|a + b|^2$; a large negative interference is apparent.
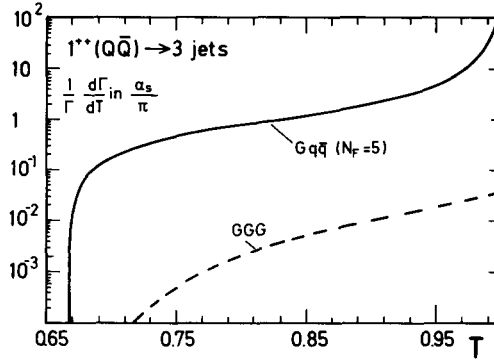
Fig. 12. Thrust distribution of $1^{++}(Q\overline{Q}) \to Gq\overline{q}$ ($N_F = 5$ light quark flavors) compared with GGG.

The presence of infrared divergences for gluon radiation from the fermion line for P-waves is due to spin. For $p_G \to 0$ the gluon emission vertex $\overline{u}\displaystyle{\not}u \propto |p_G|$. For S-waves this cancels the $|p_G| \to 0$ divergence of an attached fermion propagator. For P-waves, this $|p_G|$ factor is absorbed into the wave function[*]. The fermion propagator divergence remains. We thus expect similar trouble for $^3P_0$ and $^3P_2$ decays, though perhaps less spectacular than that encountered for $^3P_1 \to GGG$. We first discuss $^3P_0$.

$^3P_0 \to GGG + Gq\overline{q}$

We present the $a(+, + -)$ and $b(+, + -)$ amplitudes in figs. 13a,b. Again gluon radiation from the fermion line tends to cancel the diagrams with a 3G vertex. The dominant amplitudes are a$(+, + +)$ and b$(+, + +)$. (The $+ - -$ amplitudes are everywhere small[**].) In fig. 13c we show the overall thrust distribution for $^3P_0 \to$ GGG. The gluon radiation from the fermion line does produce a divergence as $T \to 1$, but its coefficient is small. The thrust distribution for 3G is dominated by diagrams with the 3G vertex. In fig. 13c we also show the $Gq\overline{q}$ final state. It is again small.

$^3P_2 \to GGG + Gq\overline{q}$

For the decay of a spin-2 state to GGG there are no angular momentum constraints on soft divergences $|p_G| \to 0$ (the remaining hard GG can have any total $|S_z| \leqslant 2$). It is therefore not surprising that almost all helicity amplitudes ($+ - +$, $+ - -$ and $+ + -$) are large. What is a bit baffling to us is the circumstance that

$$a\left(^3P_2 \to + + +\right) + b\left(^3P_2 \to + + +\right) = 0 \qquad (51)$$

(again!). Also, a and b are separately small. This does not occur for $^3P_0$. The (unrelated) thrust distributions for $+ + -$ and $+ - -$ amplitudes are shown in fig. 14. The total 3G thrust distribution is shown in fig. 15. Again, there is an infrared

---

[*] Recall the second of eqs. (19).

[**] The reason is again spin. A log divergence will arise for $x_1 \to 0$, giving an essentially GG decay. This has $S_z = \pm 2$ and must be suppressed by angular momentum barrier effects. (If x_1 is maximal the fragmentation function $G(+) \to G(-)G(-)$ vanishes in the leading log limit.)
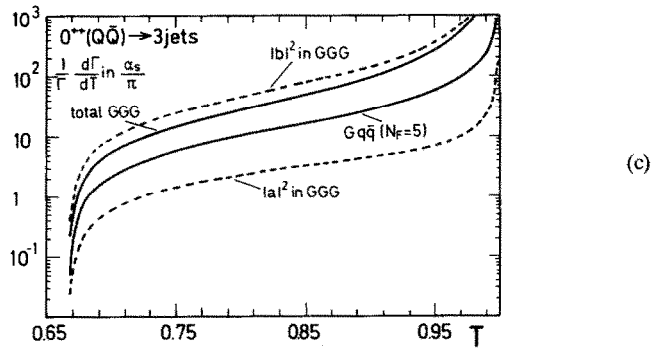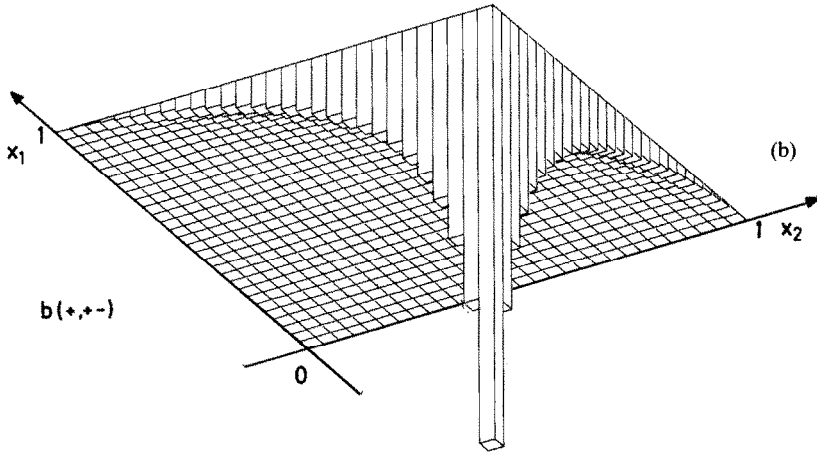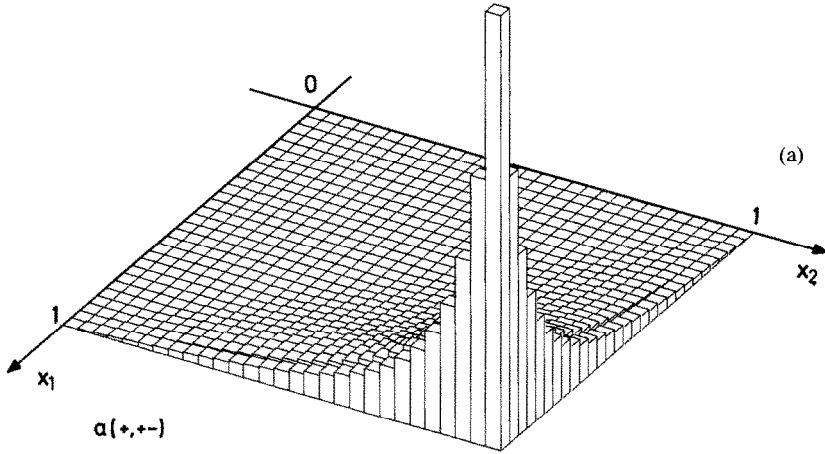
Fig. 13. (a,b) Helicity amplitudes for $0^{++} \rightarrow G(+)G(+)G(-)$; (c) thrust distribution for $0^{++} \rightarrow 3G$ in comparison with $0^{++} \rightarrow Gq\bar{q}$ ($N_F = 5$ light quark flavors)
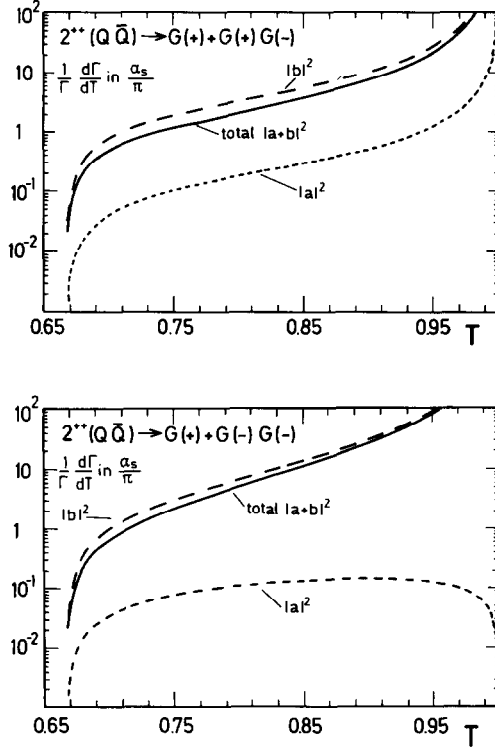
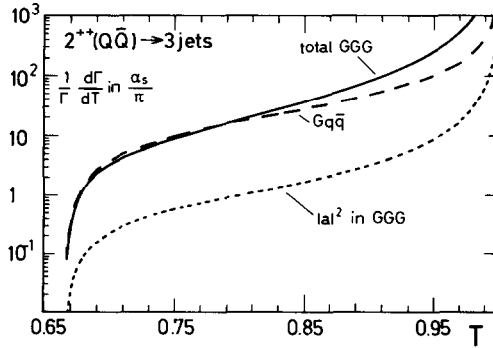Fig. 14. Thrust distributions for $2^{++} \to G(+) + G(+)G(-)$ and $2^{++} \to G(+) + G(-)G(-)$.

Fig. 15. Thrust distributions for $2^{++} \to GGG$ in comparison with $Gq\bar{q}$. Separately shown is the contribution $|a|^2$ to GGG where all gluons are attached to the heavy quark line.

divergence arising from soft gluon radiation from the heavy fermion. But it is numerically unimportant. Likewise, the $Gq\bar{q}$ final state is numerically unimportant.

6. Summary

The main aim of this work has been to calculate the three jet decays of $C = +$ quarkonia as a preliminary to the 4-jet and $\gamma + 3$-jet decays of the longingly awaited $^3S_1(t\bar{t})$ toponium state. We find that S-wave $^1S_0$ decays are well-behaved, as expected. P-wave decays are not. Most dramatic is the $^3P_1 \to GGG$ decay which almost vanishes due to cancellations [7]. ($^3P_1 \to Gq\bar{q}$ is thus dominant, as is well known.)

The $^3P_0$, $^3P_2 \to GGG + Gq\bar{q}$ decays, if observable, could serve as a way of finding the 3G vertex. One could compare

$$2^3S_1(b\bar{b}) \to \gamma + \underbrace{^3P_0 \text{ or } ^3P_2(b\bar{b})}_{\llcorner\!\!\to GGG + Gq\bar{q}} \tag{52}$$

and

$$2^3S_1(t\bar{t}) \to \gamma + \underbrace{^3P_0 \text{ or } ^3P_2(t\bar{t})}_{\llcorner\!\!\to GGG + Gq\bar{q},} \tag{53}$$

to check for jet broadening and, in the latter case, 3-jet events at a rate signalling the 3G vertex of QCD. We find that cancellations in the 3G state are present for the $^3P_0$, $^3P_2$ cases. But they are not dramatic. Amplitudes with G radiation from a fermion line – finite for S-waves – have weak infrared divergences for these P-waves. Numerically this will not interfere with jet studies in (52), (53). This is illustrated again in table 1 which summarizes the expectation values of $\langle 1 - T \rangle$ for 3-jet decays of $^1S_0$, $^3P_0$, $^3P_1$ and $^3P_2$. Separately shown are the GGG contributions of the a amplitudes with all gluons coming from the heavy quark line, the 3G vertex contributions; the entire GGG value is compared with $Gq\bar{q}$ for $N_F = 5$ light quark flavors in the final state.
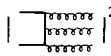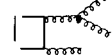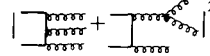
The decays (52) and (53) may be hard to see experimentally. If the experiments are possible, the three-parton matrix elements can be used as input to a two- and three-jet model. This can be compared to data to check for the three-gluon coupling. The procedure would be analogous to that in $e^+e^- \to q\bar{q}G$, which has been successful in checking the $q\bar{q}G$ matrix element [4].

Perhaps the cleanest place to study the effect of the 3G vertex on jet broadening and the 3-jet rate will turn out to be the decay

$$^3S_1(t\bar{t}) \to \gamma GG + \gamma GGG + \gamma Gq\bar{q},$$

where the kinematics is simple. Other reactions like 2-gluon bremsstrahlung in the

TABLE 1

Average values of $\langle 1 - T \rangle$ for 3-jet decays

	$\left| \begin{array}{c} \end{array} \right|^2$ (GGG $|a|^2$)	$\left| \begin{array}{c} \end{array} \right|^2$ (GGG $|b|^2$)	$\left| + \right|^2$ (GGG)	$\sum_{N_F=5} \left| \begin{array}{c} \end{array} \right|^2$ (Gq$\bar{q}$)
$^3S_1 = 1^{--}$	0.109 (absolute value)	0	0.109	0
$^3S_0 = 0^{-+}$	0.0157	2.53	2.63	0.423
$^3P_0 = 0^{++}$	0.124	3.81	2.64	0.689
$^3P_1 = 1^{++}$	0.00672	0.00660	0.000173	0.0535
$^3P_2 = 2^{++}$	0.0888	2.68	2.23	1.13

The third column shows the value for GGG decay, the first columns the $|a|^2$ and $|b|^2$ contributions separately. The Gq$\bar{q}$ value is given for 5 light quark flavors. All numbers in units of α_s/π (except 1^{--}). The final results agree within errors with those of Barbieri et al. [6]. For 1^{++} we used the width in logarithmic approximation for a 25 GeV quark.

$e^+ e^-$ continuum and large-$p_\perp$ scattering have been discussed as tests of the 3-gluon vertex as well (see e.g. ref. [16]). We will comment more thoroughly on these possibilities in our future paper on 4 jet orthoquarkonium decays.

References

[1] Y. Nambu, Preludes in theoretical physics (North-Holland, Amsterdam, 1966);
    H. Fritzsch, M. Gell-Mann and H. Leutwyler, Phys. Lett. 47B (1973) 365;
    H.D. Politzer, Phys. Rev. Lett. 30 (1973) 1346;
    D.J. Gross and F. Wilczek, Phys. Rev. D8 (1973) 3497;
    T. Appelquist and H.D. Politzer, Phys. Rev. D12 (1975) 1404;
    H.D. Politzer, Phys. Reports 14 (1974) 129;
    V.A. Novikov et al., Phys. Reports 41 (1978) 1
[2] C. Berger et al., Phys. Lett. 82B (1979) 449;
    H. Meyer, Proc. 1979 Lepton-photon symp., Fermi National Accelerator Laboratory
[3] K. Koller and H. Krasemann, Phys. Lett. 88B (1979) 119;
    T.F. Walsh and P.M. Zerwas, Phys. Lett. 93B (1980) 53
[4] R. Brandelik et al., Phys. Lett. 86B (1979) 243;
    D.P. Barber et al., Phys. Rev. Lett. 43 (1979) 830;
    C. Berger et al., Phys. Lett. 86B (1979) 418;
    W. Bartel et al., Phys. Lett. 91B (1980) 142
[5] K. Shizuya and S.-H. Tye, Phys. Rev. Lett. 41 (1978) 787 (E: 41 (1978) 1195);
    M.B. Einhorn and B.G. Weeks, Nucl. Phys. B146 (1978) 445

[6] R. Barbieri, G. Curci, E. d'Emilio and E. Remiddi, Nucl. Phys. B154 (1979) 535;
     W. Celmaster and D. Sivers, Argonne preprint PR-80-61;
     R. Barbieri, M. Caffo and E. Remiddi, Nucl. Phys. B162 (1980) 220
[7] R. Barbieri, R. Gatto and E. Remiddi, Phys. Lett. 61B (1976) 465
[8] K. Koller, T.F. Walsh and P.M. Zerwas, Phys. Lett. 82B (1979) 263
[9] G. Altarelli and G. Parisi, Nucl. Phys. B126 (1977) 298;
     T. Uematsu, Phys. Lett. 79B (1978) 97;
     J.F. Owens, Phys. Lett. 76B (1978) 85
[10] M. Jacob and G.C. Wick, Ann. of Phys. 7 (1959) 404
[11] H. Krasemann, Thesis, Hamburg University (1978)
[12] K. Koller and T.F. Walsh, Nucl. Phys. B140 (1978) 449
[13] V.A. Novikov et al., ref. [1]
[14] K. Shizuya and S.-H. Tye, Phys. Rev. D20 (1979) 1101
[15] S.J. Brodsky, T.A. DeGrand and R.F. Schwitters, Phys. Lett. 79B (1978) 255
[16] A. Ali et al., Nucl. Phys. B167 (1980) 454;
     M. Glück and E. Reya, Dortmund University preprint, DO-TH 80/11 (May, 1980)